Ionization and excitation dynamics of H(1*s*) in short intense laser pulses

J. P. Hansen,[1,*] J. Lu,[2] L. B. Madsen,[3] and H. M. Nilsen[4,*]
[1]*Foundation for Research and Technology–Hellas, IESL, P.O. Box 1527, Heraklion 71117, Crete, Greece*
[2]*Department of Physics, University of Bielefeld, D-33615 Bielefeld, Germany*
[3]*Institute of Physics and Astronomy, University of Aarhus, DK-8000 Aarhus C, Denmark*
[4]*The Queen's University of Belfast, Belfast BT7 1NN, Northern Ireland*
(Received 11 April 2001; published 17 August 2001)

We present an analysis of the ionization and excitation dynamics of H(1*s*) when exposed to an ultrashort and intense laser pulse. The studies are based on quantum close-coupling calculations and classical trajectory Monte Carlo simulations. The quantum and classical approaches are compared at three different levels: (i) Total (ii) differential ionization probabilities, and (iii) a direct comparison of the dynamics during the laser pulse from snapshots of the spatial electronic probability density. For short and intense pulses, the results of the two methods are in fair agreement. We show that the direction of ejection of the ionized electron is very asymmetric and strongly sensitive to the initial phase of the electric field.

DOI: 10.1103/PhysRevA.64.033418 PACS number(s): 32.80.Rm

I. INTRODUCTION

Notwithstanding the remarkable successes of nonrelativistic Schrödinger-like quantum mechanics in describing the physics of atoms and molecules, classical models are, as already pointed out by Bohr [1], of great value since it is only in such terms that our minds can fully comprehend (quantum) dynamical systems. Fortunately, when a quantum system, such as the hydrogen atom, interacts with a large energy reservoir, a semiclassical approximation can be derived [2] in which a classical time is introduced into the quantum system (for a recent reference, see Ref. [3]). The dynamics of the atoms is then described by the interaction with the classical dynamical variables of the energy reservoir, i.e., a laser field or an energetic heavy particle. A remaining and open question is then, to which extent also the atomic dynamics can be described by classical mechanics based on an ensemble of classical electrons (CTMC - Classical Trajectory Monte Carlo method) interacting with the atomic Coulomb potential and the external time-dependent energy reservoir.

This question has been answered for the highly excited Rydberg states, and is in this case expressed in terms of the correspondence principle [4,5], which states that the predictions of classical and quantum mechanics should merge in the limit of high quantum numbers. Since the initial work by Bohr [4], which successfully lead to the correct prediction of the Rydberg constant, the correspondence principle has been studied in great detail and formulated in several ways [5]. Here we investigate the correspondence between classical and quantum dynamics for *tightly bound* states exposed to a rapid strong perturber, taken to be an ultrashort intense laser pulse.

In collision physics, a range of fundamental mechanisms have a classical analogy. Most well known is perhaps the Thomas scattering mechanism from 1927 [6], where the capture process is described in terms of two sequential binary collisions leading to electron-capture at certain angles. This process was described quantum mechanically in Ref. [7] and first measured in Ref. [8]. We mention also electron-capture processes from oriented Rydberg atoms, where oscillations in the capture cross sections have been interpreted by the so-called *n* swaps [9]. In this model the oscillations of the capture cross sections are found to originate from electron trajectories crossing the midplane between the projectile and the target one, three, five, $\ldots, 2n+1$ times. This process has however not been described by quantum theory, and indeed the swapping mechanism is found to be invalid for transfer processes from ground-state atoms [10]. Finally, we mention that the CTMC method has described the main features of the quantal and experimental differential cross sections for capture from initially oriented Na($3p$) atoms [11,12], and many excellent agreements between CTMC calculations for breakup and ionization of many-electron systems have been obtained (see, e.g., Ref. [13]).

Semiclassical models [14–16] have also been useful in describing strong-field laser-atom interactions. In particular, a rescattering mechanism has been discussed extensively in connection with above-threshold ionization, high-harmonic generation, and ''enhanced'' double ionization by short pulses (see, Ref. [17] for an early reference and Ref. [18] for a recent review). In particular, this mechanism has been able to predict the plateau and cutoff regions. We would like to stress that this rescattering model is not purely classical: Even in its simple form [17] certain quantum-mechanical elements of, e.g., the ionization process are invoked. In other formulations [19] the term rescattering is introduced in order to describe the effect of the inclusion of an additional term in a field-dressed quantum-mechanical Born-like series for the interaction between the atom and the field.

Ionization of Rydberg atoms by short half-cycle pulses was studied recently [20], and the results were found to lie on a universal classical scaling-invariant curve [21,22]. The investigations explored the region where the duration of the pulse is shorter or comparable to the classical orbital period T_n. For recent references on pulsed-field ionization of Rydberg atoms including CTMC studies, see the works of Ro-

*Permanent address: Institute of Physics, University of Bergen, Allégaten 55, N-5007 Bergen, Norway.

bicheaux [23]. In general quite good agreement between quantum and classical calculations was found. Very recently Cormier and co-workers have conducted work on hydrogen, related to ours, but at much higher intensities (above the atomic unit of intensity, $I_0=3.51\times10^{16}$ W/cm^2) and at much lower laser frequency ($\omega=0.05$ a.u.) [24,25]. In this impulsive regime, they did find that the CTMC and quantum predictions compare rather well for very short 5 a.u. and 10 a.u. pulses, also for the photoelectron-energy spectrum [25].

In this work, we perform a study of the ionization of the H($1s$) ground state for values of the pulse length to orbital period similar to the ones considered in the half-cycle-pulse studies mentioned above. As a consequence of the scaling with the principal quantum number, this means much shorter pulses and much larger frequencies. Compared to the Rydberg studies, the present work exposes the more quantum-mechanical nature of the $1s$ state. Explicitly, we shall compare the microcanonical CTMC method with *ab initio* quantum-mechanical close-coupling calculations of H($1s$) under an intense laser pulse of short duration. The purpose of the paper is twofold: First, we address the fundamental question of classical versus quantum description of the ionization dynamics at laser intensities, low enough such that ''over the barrier'' ionization is classically allowed only for a fraction of the laser pulse. Excited states are thus important intermediate states and the Coloumb potential plays a decisive role in the ejection process in contrast to Ref. [25]. Second, we explore the possibility of predicting new measurable quantities from future experimental sources. We note that the requirements on pulse durations and intensities for the laser source to be considered in the following, should be within experimental reach in the not to distant future [26,27]. Multigigawatt 4.5 fs laser pulses operated at 800 nm have recently been achieved [28], not to mention the exciting developments of accelerator-based bright coherent sources extending into the uv and x-ray regimes.

Geltman [29] has recently performed a comprehensive study of ionization from H($1s$) based on quantum calculations with much smaller basis sets than we present here. In the present work we will adopt the pulse shape and laser frequencies considered by Geltman. Earlier, in particular, Lambropoulos and co-workers (see Ref. [18], and references therein) have developed the *B*-spline theory for H($1s$) ionization and performed calculations of both ionization probabilities as well as differential spectra.

This paper is organized as follows. In Sec. II we present the quantum (Sec. II A) and the classical (Sec. II B) theory. In Sec. III, we present our results and discuss in detail differences and similarities between the classical and quantum predictions for total and differential probabilities at the detailed level of the time development of the electron probability density.

II. THEORY

A. Quantum close coupling

We aim to solve the time-dependent Schrödinger equation for the hydrogen atom (atomic units [a.u.] are used throughout unless otherwise specified),

$$\left(-\frac{1}{2}\nabla^2-\frac{1}{r}+\vec{r}\cdot\vec{E}(t)-i\frac{\partial}{\partial t}\right)\Psi(\vec{r},t)=0. \tag{1}$$

The laser field is assumed to be accurately described by a time-dependent electric field

$$\vec{E}(t)=\vec{E}_0\sin^2\left(\frac{\pi}{2}\frac{t}{T}\right)\cos(\omega_L t) \tag{2}$$

of pulse duration $2T$ and with laser frequency ω_L. Only linear polarized light, $\vec{E}_0=E_0\vec{e}_z$, will be considered in the following. The $\sin^2$ part of Eq. (2) describes the temporal envelop of the pulse. Focusing effects, not to be considered here, can be accounted for by introducing an additional spatial envelope function into Eq. (2).

We expand the wave function in a set of field-free eigenstates describing the bound-state spectrum and a discretized continuum, constructed by solving the problem in a suitable large box,

$$\Psi(\vec{r},t)=\sum_{n=1}^{n_{max}}\sum_{l=0}^{n-1}a_{n,l}(t)R_{n,l}(r)Y_{l,m=0}(\hat{r}) + \sum_{k_i=0}^{k_{max}}\sum_{l=0}^{L_{max}}b_{k_i,l}(t)\Phi_{k_i,l}(r)Y_{l,m=0}(\hat{r}). \tag{3}$$

Here $R_{n,l}$ and $Y_{l,m=0}$ are the well-known radial and angular eigenfunctions of hydrogen. Only the magnetic quantum number $m=0$ needs to be considered due to the conservation of $\vec{E}_0\cdot\vec{L}$ and the choice of the spherically symmetric $1s$ initial state. The continuum functions are built up by those radial functions that vanish at the end of the chosen box. Since this number of functions may be extremely large for box sizes $r_b\sim1000$, we apply the so-called eigendifferentials. Various related methods of this type have been used in atomic and nuclear collisions [30–32] and it was recently also introduced to laser-atom interactions [33]. In the present approach, the set of continuum functions satisfying $R_{k_i,l}(r_b)=0$ are first normalized and then grouped into smaller sets,

$$\Phi_{k_i,l}(r)=\frac{1}{\sqrt{2N+1}}\sum_{j=i-N}^{i+N}R_{k_j,l}(r). \tag{4}$$

This procedure decreases the number of basis-set wave functions by a factor of $2N+1$ while the boundary condition is maintained. Furthermore, the present method gives an equidistant mesh of states in k space, which is ideal for laser pulses of short duration. Since the discrete basis functions form an orthonormal set, the inclusion of Eq. (3) into Eq. (1) leads to a set of first-order coupled equations,

$$i\frac{d}{dt}\vec{c}=\mathbf{H}(t)\vec{c}, \tag{5}$$

where the vector $\vec{c}=(\vec{a},\vec{b})$ is the collection of expansion coefficients and where the coupling matrix $\mathbf{H}(t)$ contains the

field-free energies on the diagonal and nonzero dipole-coupling matrix elements for states with $\Delta l = \pm 1$.

Any observable may be derived from the amplitude vector $\vec{c}$ after integration from $t=0$ to $t_f = 2T$. The total excitation probability is given by

$$P_e = \sum_{n=2}^{n_{max}} \sum_{l=0}^{n-1} |a_{n,l}(t_f)|^2. \tag{6}$$

The angle-integrated ionization probability for an electron with energy $E_i = \frac{1}{2}k_i^2$ is given by

$$\frac{dP}{dE_i} = \sum_{l=0}^{L_{max}} |b_{k_i,l}(t_f)|^2 \tag{7}$$

and the total ionization probability is

$$P_i = \sum_{k_i} \frac{dP}{dE_i}. \tag{8}$$

Finally, the angular distribution is given by [34]

$$\frac{dP}{d\theta} \propto \sum_{k_i} \left| \sum_l (-i)^l b_{k_i,l}(t_f) e^{i\delta_l} Y_{l,0}(\theta) \right|^2, \tag{9}$$

where δ_l is the Coulomb phase shift. At the most detailed level, we will study the time development of the spatial electron probability density,

$$\rho_{QM}(x,y,z,t) = \langle \delta(\vec{r},t) \rangle = |\Psi(\vec{r},t)|^2, \tag{10}$$

where the wave function $\Psi(\vec{r},t)$ is given by Eq. (3). Because of the rotational symmetry of the problem a cut for $y=0$ carries all information about probability density at a given instant of time.

The present method requires a careful testing of the basis size with respect to the limiting parameters. For the physical processes considered here, we have obtained convergence within a few percent by setting $(n_{max}, L_{max}, r_b, E_{max} = \frac{1}{2}k_{max}^2, N) = (15,24,1000,1.7,5)$. Smaller basis sets, resulting from other choices of these parameters, do not change the final probabilities significantly. The present basis thus amounts to 120 discrete and 2816 continuum states coupled by 330 906 nonzero dipole matrix elements. The basis span a dense mesh up to $E_{max} = 1.7$ a.u.. Longer pulse lengths than considered here would, for high intensities, certainly require higher-energy states in resonance with n-photon transitions. These could, in principle, be introduced at the expense of a large number of continuum states corresponding to the present uniform k-space distribution in the continuum, cf. Ref. [29].

B. Classical trajectory Monte Carlo

The CTMC calculations are based on the solution of Newton's equation of motion

$$\mu \frac{d^2}{dt^2}\vec{r}(t) = -\frac{\vec{e}_r}{r^2} - \vec{E}(t) \tag{11}$$

for the position $\vec{r}(t)$ of an electron with reduced mass μ. This equation is integrated from $t=0$ to $t=t_f$ for a large number of trajectories ($\sim 10^5$) corresponding to different initial conditions picked at random from a microcanonical ensemble, cf. Ref. [35]. In short, the initial values of the position and momentum are given by five uniformly distributed quantities,

$$\beta \in [0, \beta(r_{\max})], \quad \varphi_r \in [0, 2\pi], \quad \varphi_p \in [0, 2\pi] \tag{12}$$

$$v_r \in [-1, 1],$$

and

$$v_p \in [-1, 1],$$

since the constraint $E = -1/2$ a.u. fixes the last degree of freedom. The initial values of position and momentum are now defined by

$$x = r(1 - v_r^2)^{1/2} \cos\varphi_r, \tag{13}$$

$$y = r(1 - v_r^2)^{1/2} \sin\varphi_r, \tag{14}$$

$$z = r v_r, \tag{15}$$

$$p_x = \left(2\mu \left[E + \frac{1}{r} \right] \right)^{1/2} (1 - v_p^2)^{1/2} \cos\varphi_p, \tag{16}$$

$$p_y = \left(2\mu \left[E + \frac{1}{r} \right] \right)^{1/2} (1 - v_p^2)^{1/2} \sin\varphi_p, \tag{17}$$

$$p_z = \left(2\mu \left[E + \frac{1}{r} \right] \right)^{1/2} v_p. \tag{18}$$

Here the quantity β is related to r through the transformation

$$\beta(r) = \int_0^r dr' \mu r'^2 \sqrt{2\mu \left(E + \frac{1}{r'} \right)}, \tag{19}$$

which can be straightforwardly integrated analytically or numerically. After the pulse, an ionized electron is identified by a positive energy. For excitation, i.e., for electrons with a final energy $-1/2 < E_f < 0$, a certain binning procedure has to be applied to allocate a classical principal quantum number $n_{cl} = \sqrt{1/(-2E_f)}$ to a quantal quantum number n. We follow the widely used procedure [11], and chose

$$\left[(n-1)\left(n - \frac{1}{2} \right) n \right]^{1/3} \leq n_{cl} \leq \left[n\left(n + \frac{1}{2} \right)(n+1) \right]^{1/3}. \tag{20}$$

Corresponding to the quantum-mechanical density of Eq. (10), we calculate a classical density ρ_{Cl}: Define $N_{i,j}$ as the number of particles at a given time in the (cylindrical) region of the configuration space given by

$$z_i - dz \leq z < z_i + dz,$$

$$r_j - dr \leq r < r_j + dr, \tag{21}$$

$$r=\sqrt{x^2+y^2},$$

and let

$$V_{i,j}=8\pi r_j dr dz \tag{22}$$

be its volume. In terms of $N_{i,j}, V_{i,j}$ and the total number of particles N_{all} the CTMC probability is then given by

$$\rho_{Cl}(r_j,z_i;t)=\frac{1}{V_{i,j}}\frac{N_{i,j}}{N_{all}}. \tag{23}$$

This probability is the classical quantity corresponding to the quantal Eq. (10). The uncertainty in the present CTMC calculations is estimated to be below 1% for the main channels.

III. DISCUSSION AND RESULTS

In discussing our results, it is convenient to consider the dimensionless scaling variables, which keep the classical equations of motion invariant [5] $\vec{r}'(t')=\alpha\vec{r}(t),\ t'=\alpha^{3/2}t$, where α is a positive scale factor. In particular, we consider, the ratio T_0 of the pulse length T_p to the classical orbital period T_n. For the $1s$ state considered here, $T_{n=1}=2\pi$ and $T_0=T_p/2\pi$. In the half-cycle-pulse studies of Refs. [20–22], the value of T_0 was varied by changing the degree of excitation of the Rydberg state and the interval $10^{-2}<T_0<10^1$ was scanned through, and a good agreement between quantum and classical results was found for the Rydberg states. Here we shall consider essentially the same range of T_0, but by varying the pulse length and placing the hydrogen atom initially in the ground state. From the point of view of the correspondence principle, we are certainly not in the regime of high quantum numbers, nevertheless, the quantum and classical results may be compared in order to explore classical features of the dynamics.

A. Total ionization and excitation probability

Figure 1 shows the total ionization probabilities as a function of pulse length for two different values of the field strength, $E_0=0.33$ and $E_0=0.05$. The upper and lower panels are for laser frequencies corresponding to $\omega_L=0.55$ a.u. and $\omega_L=0.18$ a.u., respectively. These frequencies place the studies in the one- and three-photon ionization regimes. Both panels show a good quantitative agreement with the $E_0=0.05$ results of Geltman [29]. This represents an independent check of the convergence of the present results and lends additional confidence to the method used. We note some minor discrepancies with Geltman at the shortest pulse lengths where his results oscillates weakly around ours. We believe these oscillations are an artifact of the much smaller basis used in Ref. [29]. A more serious discrepancy is observed for $\omega_L=0.18$ for the longer pulse lengths, where our probabilities are a factor of 2 larger than Geltman's. New and independent calculations are needed to resolve this divergence. Although not shown, we mention that for lower intensities, we obtain indeed very good agreement with the results of Geltman. In particular, we reproduce the large drop in the ionization probability for $\omega_L=0.18$ and $E=10^{-3}$ when the pulse length goes from ~ 0.1 to ~ 0.3 (see Fig. 3 in Ref. [29]). The origin of such nonmonotonic behavior of the ionization probability is to be found in the delicate interplay between couplings of states and the time scales involved.

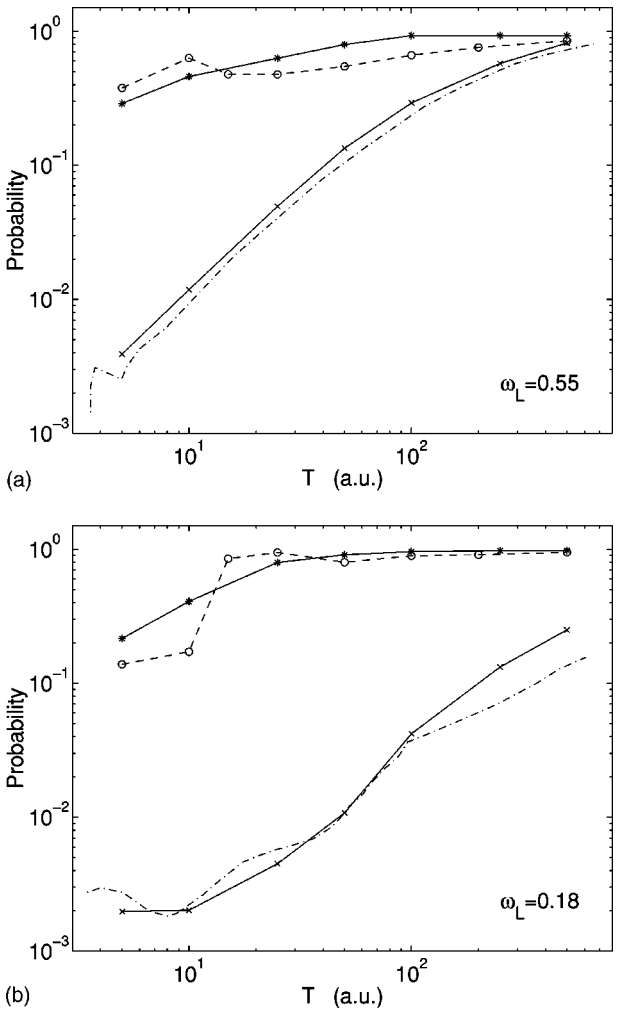

FIG. 1. Ionization probabilities as function of pulse length for two different intensities. Upper, $\omega_L=0.55$: $E_0=0.33$(—*—) present quantal calculations, $E_0=0.33$(—o—) present classical calculations, $E_0=0.05$(—×—) present quantal calculations, $E_0=0.05$(- - - -) quantal calculations by Geltman [29]. The lower panel shows the corresponding results for $\omega_L=0.18$.

The curves shown by —*— and —o— in Fig. 1 correspond to the quantum and classical calculation for the two frequencies. We observe a qualitative overall agreement between the two approaches for the entire span of pulse lengths: The classical theory accounts fairly accurately for the total ionization of the strongly bound $1s$ quantum state, in the sudden ($T_p \ll 1$), intermediate ($T_p \simeq 1$), and adiabatic ($T_p \gg 1$) regimes. This is, however, true only for the case of the strong field $E_0=0.33$. For a weaker perturber, $E_0=0.05$, notably still a rather strong field, the classical prediction breaks completely down and underestimates the probabilities by several orders of magnitude. To keep the figures clear and the discussion focused, we have chosen not to show these CTMC results.

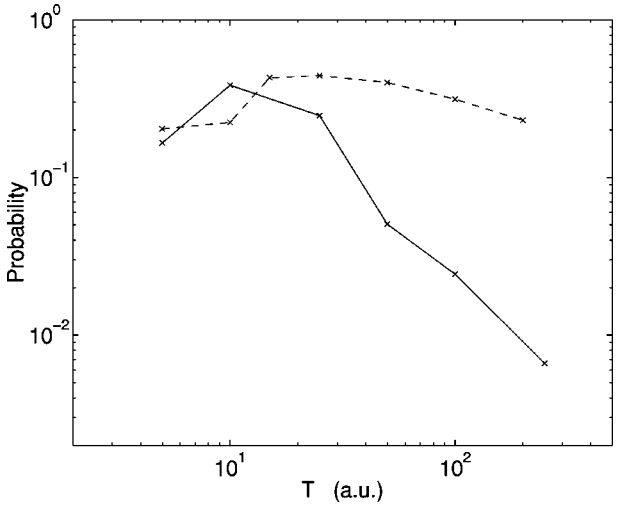

FIG. 2. Excitation probability as function of pulse length for $\omega_L=0.55$, $E_0=0.33$; (—×—) quantal calculations, (- -o- -) classical calculations.

Figure 2 shows the excitation probability as a function of pulse length for the bound-state part of the spectrum for the strong field ($E_0=0.33$) and high frequency ($\omega_L=0.55$). In the sudden and intermediate regimes, the quantum and classical calculations agree within a factor of 2. For the longer pulse lengths corresponding to the $T_p \gg T_1$ (adiabatic) regime, the excitation probability is much smaller in the quantum than in the classical case. Comparing with Fig. 1, we conclude that much more of the population stays in the 1*s* ground state as the pulse length increases in the quantum-mechanical calculation. This is due to the decrease in the Fourier bandwidth of the laser source: For the longer pulses direct ionization to the continuum is favored compared to nonresonant bound-state excitations. These finding are also in accordance with the conventional understanding of the adiabatic limit in quantum theory (see, e.g., the book of Schiff [36]): The part of the 1*s* wave function that does not leak out into the continuum has time to adjust to the field and is not nonresonantly excited.

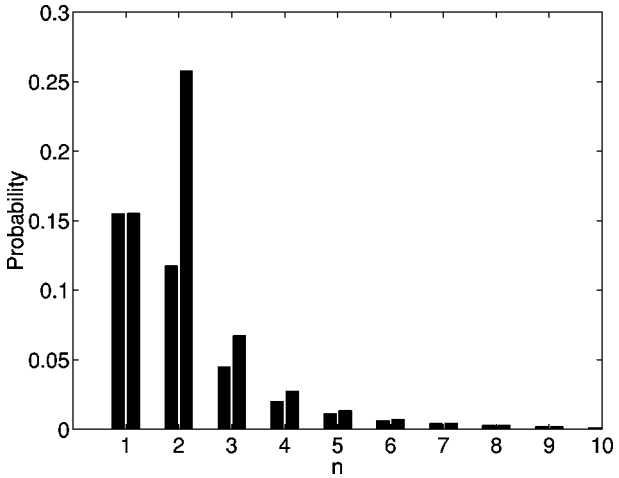

FIG. 3. Final *n*-level probabilities for a laser pulse defined by $T=10$, $\omega_L=0.55$, $E_0=0.33$. Left bars, classical results; right bars, quantal results.

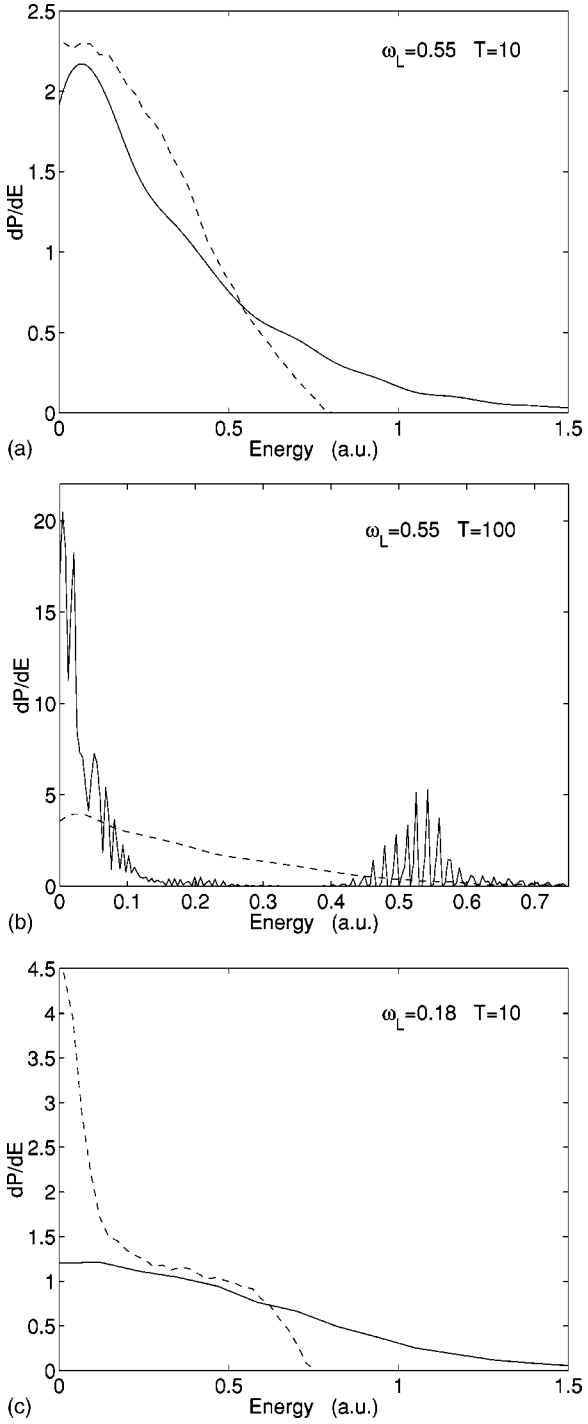

FIG. 4. Angle-integrated electron-ionization spectrum for three chosen laser frequencies and pulse lengths. Each spectrum is normalized to unit probability. (—) quantal calculations, (- - - -) CTMC calculations. Upper: $\omega_L=0.55$, $E_0=0.33$, $T=10$. Middle: $\omega_L=0.55$, $E_0=0.33$, $T=100$. Lower: $\omega_L=0.18$, $E_0=0.33$, $T=10$.

B. Differential probabilities

We now focus on differential quantities at selected pulse lengths and frequencies. Figure 3 shows the *n*-level prob-

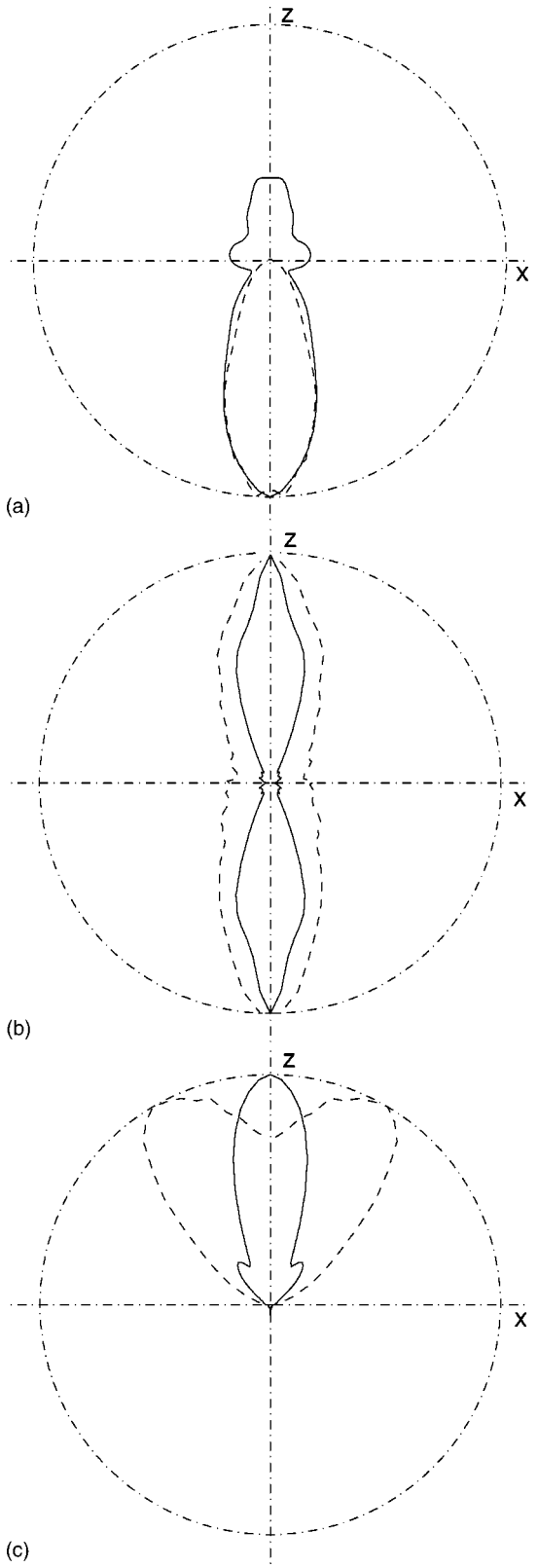

FIG. 5. Angular distributions for the photoelectron for three chosen laser frequencies and pulse lengths. Each spectrum is normalized to max value. The forward direction is marked "z" (polar angle 0°) and the perpendicular direction by "x" (polar angle 90°); (—) quantal calculations, (- - - -) CTMC calculations. Upper: $\omega_L=0.55$, $E_0=0.33$, $T=10$. Middle: $\omega_L=0.55$, $E_0=0.33$, $T=100$. Lower: $\omega_L=0.18$, $E_0=0.33$, $T=10$.

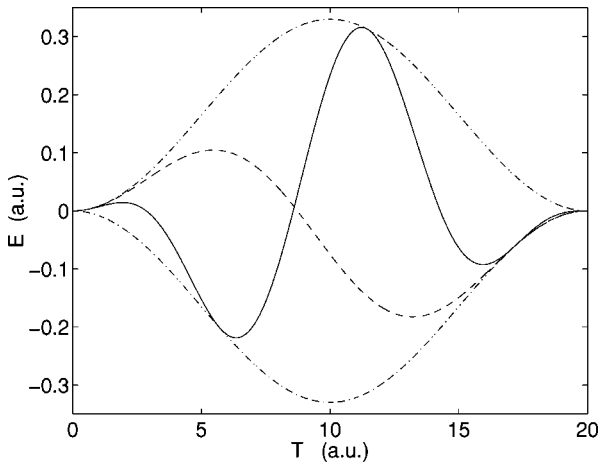

FIG. 6. The pulse for $E_0=0.33$, $T=10$, and $\omega_L=0.55$ (—) and $\omega_L=0.18$ (----). The dotted-dashed curves show the temporal envelope of the pulse.

abilities for a laser pulse defined by $T=10$, $\omega_L=0.55$, $E_0=0.33$. The left bars show the classical results and the right bars show the quantal results. The populations follow the same trend and differ most for $n=2$, which is clearly more excited in the quantum than in the classical case. This explains the difference in the excitation populations in Fig. 2 at $T=10$. The broad population of states is due to the "white" character of the frequency spectrum of the very short pulse under concern.

The three panels of Fig. 4 show normalized angular-integrated photoelectron-energy spectra, cf. Eq. (8), at $E_0=0.33$ for the two laser frequencies and for pulse durations T displayed in the upper right corners of the figures. In the upper panel, the agreement between the classical and quantum results is quite satisfactory. The peak is at approximately $\omega_L-1/2$, and the spectrum extends to an energy consistent with the bandwidth of the short-pulsed source.

The middle panel is for the longer pulse of $T=100$. Here we observe a marked difference between the classical and quantum results. The pulse is now so long that the quantized nature of the light becomes important and, of course, there is no way a classical theory can account for this. The two peaks in the quantum-mechanical photoelectron spectrum correspond to the case of one- and two-photon absorption, respectively. The ionization peaks are however shifted a little down from the resonance positions (0.05 and 0.5 for one-and two-photon ionization, respectively). This shift is due to the laser-induced ac Stark shift of the threshold, which is equal to the ponderomotive shift: The average energy of a free electron oscillating in the electromagnetic field. In the figure, we also note the narrow oscillating substructures of the photoelectron peaks. We interpret these as due to quantum interference between electrons emitted during the pulse at different energies and instants of time. Such structures were first investigated in Ref. [37] and were originally thought primarily to occur at the high-energy side of the photoelectron peaks. However, for short and strong pulses they may occur more uniformly across the peak, as seen in our figure (see also Fig. 4 in Ref. [37] and Fig. 2 in Ref. [38]).

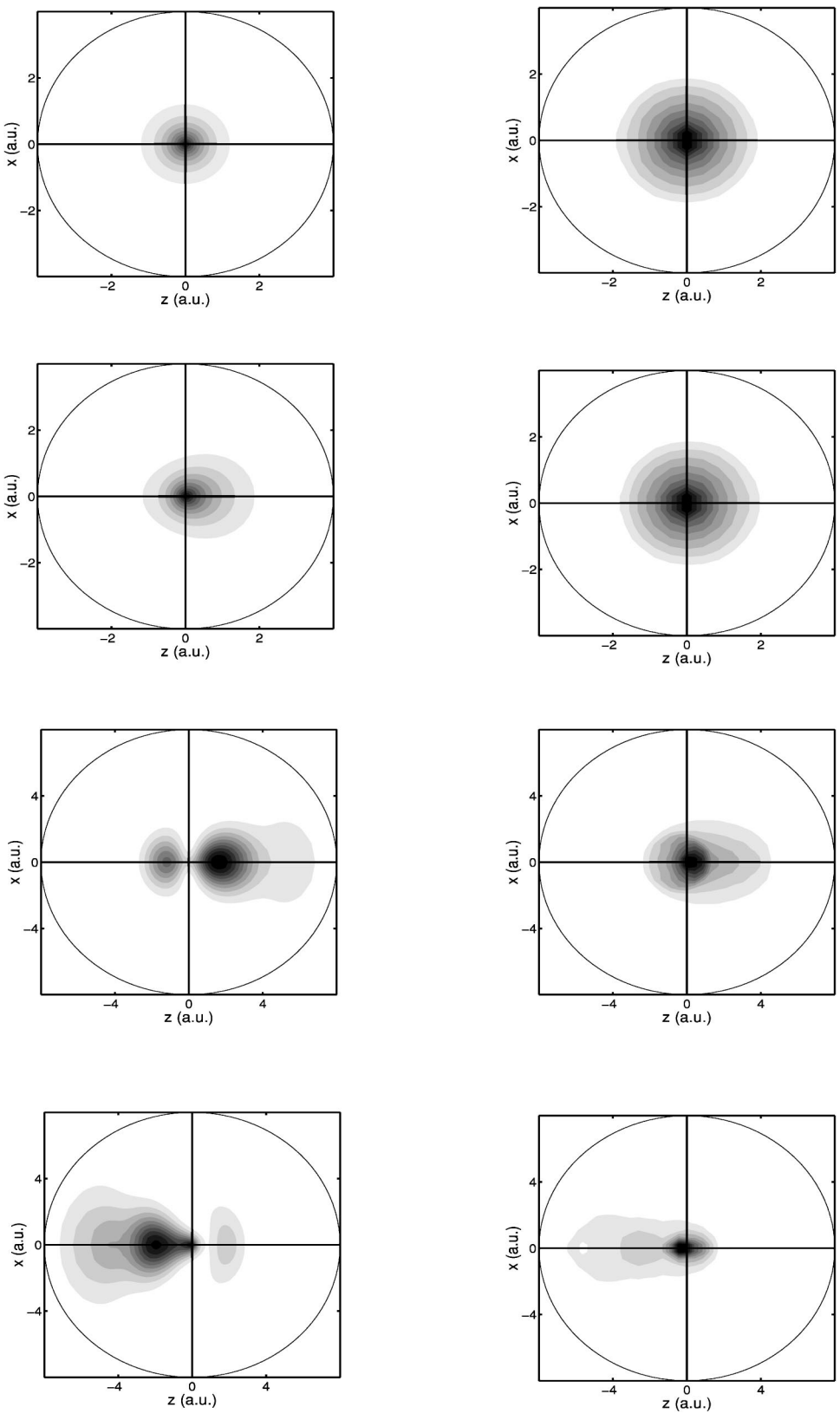

FIG. 7. Snapshots of the electron spatial probability density in the x-z plane at $t=0,1/4,1/2,3/4$ of the pulse defined by $T=10$, $\omega_L=0.55$, $E_0=0.33$. Left, quantal; right, CTMC.

Finally in Fig. 4, the lower panel shows the result for the short $T=10$ pulse in the three-photon ionization regime ($\omega_L=0.18$). Now, the results differ substantially. This is taken as a signature of the importance of the multiphoton character of the ionization process at the considered intensity. Note in passing that CTMC calculations were found to describe the ionization of hydrogen accurately at $\omega_L=0.05$ (11-photon ionization), but at much higher intensities (impulsive regime) [25]. The momentum transfer from the field to the electron as given by

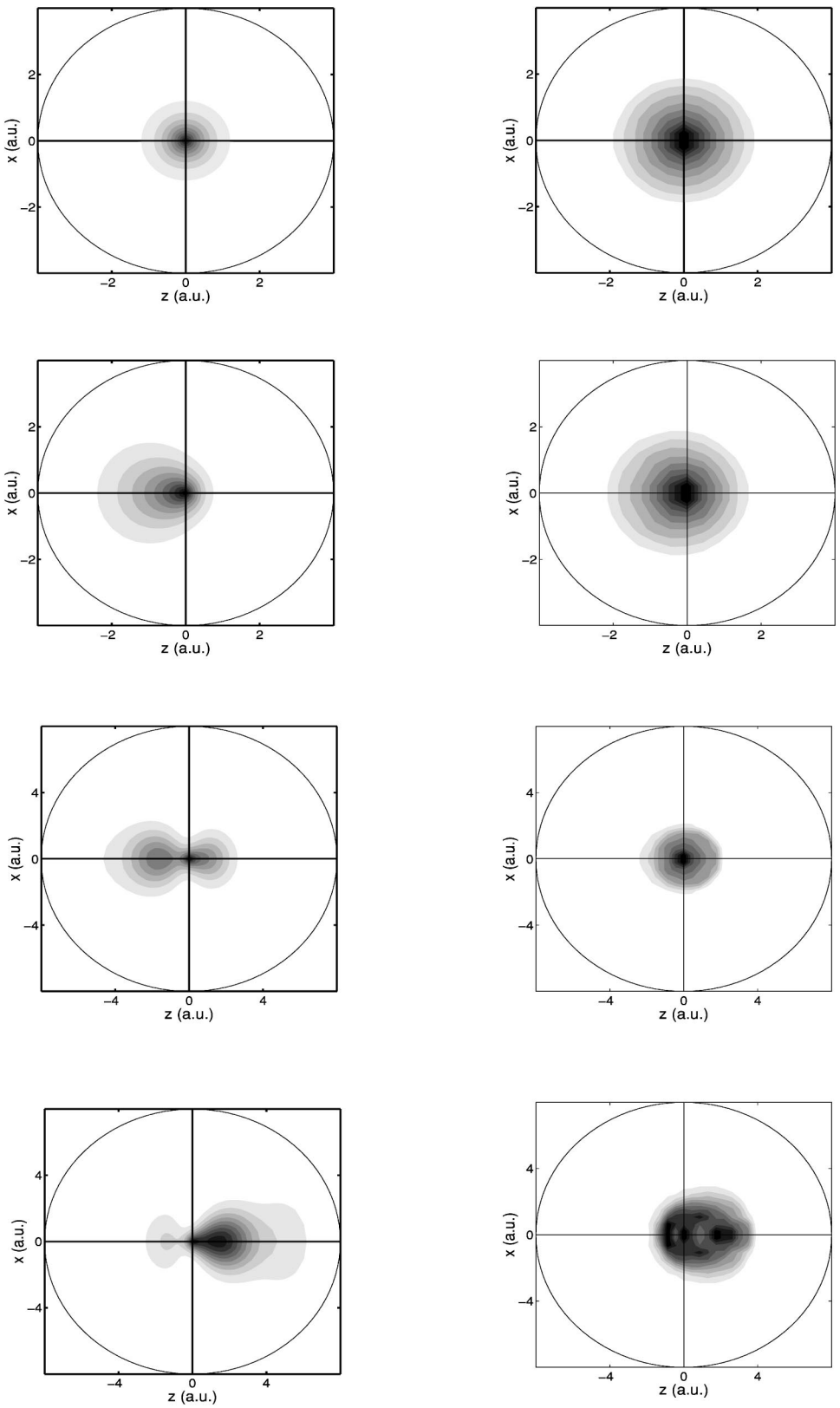

FIG. 8. Snapshots of the electron spatial probability density in the x-z plane at $t=0,1/4,1/2,3/4$ of the pulse defined by $T=10$, $\omega_L=0.18$, $E_0=0.33$. Left, quantal; right, CTMC.

$$\vec{Q}=\int_0^{2T} dt\vec{E}(t)=\frac{\vec{E}_0}{2}\frac{\sin 2\omega_L T}{\omega_L}\left\{1-\frac{1}{1-(\pi/\omega_L T)}\right\} \tag{24}$$

is, in all cases considered here, too small ($Q<1$) to kick out the electron impulsively (in the case $\pi/\omega_L \simeq 1$ a limiting procedure gives $\vec{Q}=\vec{E}_0/4$).

Figure 5 shows the angular distribution, cf. Eq. (9), of the electron for the same parameters as in Fig. 4. The short pulses (top and bottom) are seen to lead to a localized dis-

tribution in the forward and backward direction for $\omega_L = 0.55$ and $\omega_L = 0.18$, respectively. In the $\omega_L = 0.18$ case the classical distribution is significantly broader than for $\omega_L = 0.55$. Thus again, as for the energy distribution, the classical method shows a larger discrepancy with the quantal method for the less energetic photons. In general, both electron distributions are localized in either the forward or the backward direction, a distinct feature of the short pulse with only very few optical cycles. This reflects a relation between the direction of ejection of the photoelectron and the initial phase of the field. Similar effects were first discussed by Cormier and Lambropoulos [39] and subsequently by Corkum and co-workers [40]. For the long pulse (middle panel) the electron experiences more cycles of the field and a forward/backward symmetry is obtained, consistent with earlier above-threshold-ionization spectra (see, e.g., Ref. [18], and references therein). In the figure, the classical distribution is a little to broad. In particular, the electron emission perpendicular to the field is overestimated.

C. Time development

In this section, we discuss the dynamics leading to the $T = 10$ differential spectra of the preceding section. The figures are based on snapshots of the quantal and classical probability density, cf. Eqs. (10) and (23), taken at selected instants of time. Full interactive movies are available on the world wide web [41]. For clarity of the discussion we first show in Fig. 6 the electric field of the short $T = 10$ strong $E_0 = 0.33$ pulse experienced by the electron as a function of time for the two frequencies. Due to the $\sin^2$ factor of the pulse [see Eq. (2)], the field is suppressed at the beginning and end of the pulse and the effective interaction with the field corresponds very closely to one period for both frequencies. Figures 7 and 8 show snapshots of quantum and CTMC electronic probability distributions at different instants of time during the short pulse.

In Fig. 7 the classical and quantal densities are seen to have been moved to the right (2nd and 3rd rows) as the force of the electron in this period is along the positive z direction. Following the sign change of the force after $T = 10$, the densities are seen to be accelerated in the opposite direction leading to backward ionization. In the quantal dynamics however, a part of the charge cloud is unable to follow the fast change in the field, which leads to a certain fraction of electron ejection in the forward direction. Figure 8 shows the corresponding time development for the $\omega_L = 0.18$ pulse. Here the force during the important times has the opposite sign as compared to the $\omega_L = 0.55$ pulse. As a result, the electron is ejected mainly in the forward direction. A detailed comparison between the classical and the quantal densities shows larger differences. In particular the classical dynamics gives rise to a charge distribution, which is less focused in the forward direction than in the quantum-mechanical case. The excitation-rescattering dynamics is, however, still present in the classical time development, fully in accordance with the direction of the force, cf. Fig. 6. The results also show that there is a very intimate connection between the initial phase of the electromagnetic pulse and the direction of propagation of the ionized electron. In fact, it is clear that the angular distribution of the photoelectrons provides an indirect measure of the phase of the short pulse, a quantity that is not easily determined otherwise.

IV. CONCLUSION

In the present paper we have carried out close-coupling calculations of H(1s) ionization and excitation for short and intense pulses and have compared them with previous calculations [29] and classical physics. Our parallel study of the quantum and classical dynamics of H(1s) in an intense ultrashort laser pulse have shown that the classical trajectory Monte Carlo method does grasp the main features of the collision dynamics for short pulses even for such a tightly bound system when the total ionization probability is considered. For differential quantities such as the photoelectron spectrum or the angular distribution, the classical predictions are generally of lower quality. For laser frequencies well below the one-photon ionization limit, for longer pulses, and for weaker fields, the quantized nature of the light dominates and large discrepancies between differential quantities from classical and quantal mechanics appear. In conclusion, classical methods needs to be applied with great care for quantitative predictions of laser–ground-state-atom interactions when the intensity of the field is below 1 a.u.

ACKNOWLEDGMENTS

This research was supported by a Steno-talent stipendium (Grant No. 51-00-0569) from the Danish Natural Science Research Council (L.B.M.), by the Norwegian Research Council (H.M.N.), by the Deutsche Forschungsgemeinschaft (DFG) (J.L.), and by EU Project Nos. HPRI-CT-1999-00094 and HPMFCT-2000-00686.

[1] N. Bohr, in *Sources of Quantum Mechanics*, edited by B. L. van der Waerdan (Dover, New York, 1967), p. 95.
[2] J. Bang and J.M. Hansteen, Mat. Fys. Medd. K. Dan. Vidensk. Selsk. **31**, 13 (1959).
[3] J.S. Briggs and J.M. Rost, Eur. Phys. J. D **10**, 311 (2000).
[4] N. Bohr, Philos. Mag. **26**, 2 (1913).
[5] I.C. Percival and D. Richards, Adv. At. Mol. Phys. **11**, 1 (1975).
[6] L.H. Thomas, Proc. R. Soc. London, Ser. A **114**, 561 (1927).
[7] J.S. Briggs and K. Taulbjerg, J. Phys. B **12**, 2565 (1979).
[8] E. Horsdal-Pedersen, C.L. Cocke, and M. Stockli, Phys. Rev. Lett. **50**, 1910 (1983).
[9] K.B. MacAdam, J.C. Day, J.C. Aguilar, D.M. Homan, A.D. MacKellar, and M.J. Cavagnero, Phys. Rev. Lett. **75**, 1723 (1995).
[10] J.P. Hansen, L. Kocbach, S.A. Synnes, J.B. Wang, and A. Dubois, Phys. Rev. A **57**, R4082 (1998).
[11] A. Dubois and J.P. Hansen, J. Phys. B **29**, L225 (1996).

[12] A. Dubois, S.E. Nielsen, and J.P. Hansen, J. Phys. B **26**, 705 (1993).
[13] R.D. DuBois, I. Ali, C.L. Cocke, C.R. Feeler, and R.E. Olson Phys. Rev. A **62**, 060701(R) (2000); F. Frémont, C. Bedouet, M. Tarisien, L. Adoui, A. Cassimi, A. Dubois, J.-Y. Chesnel, and X. Husson, J. Phys. B **33**, L249 (2000).
[14] M. Lewenstein, Ph. Balcou, M. Yu. Ivanov, A. L'Hullier, and P.B. Corkum, Phys. Rev. A **49**, 2117 (1994).
[15] G. van de Sand and J.M. Rost, Phys. Rev. Lett. **83**, 524 (1999).
[16] G. van de Sand and J.M. Rost, Phys. Rev. A **62**, 053403 (2000).
[17] P.B. Corkum, Phys. Rev. Lett. **71**, 1994 (1993).
[18] P. Lambropoulos, P. Maragakis, and Jian Zhang, Phys. Rep. **305**, 203 (1998).
[19] F.H.M. Faisal and A. Becker, in *Multiphoton Processes 1996*, edited by P. Lambropolous and H. Walther, IOP Conf. Proc. No. 154 (Institute of Physics, London, 1997), p. 118.
[20] R.R. Jones, D. You, and P. Bucksbaum, Phys. Rev. Lett. **70**, 1236 (1993).
[21] C.O. Reinhold, M. Melles, and J. Burgdörfer, Phys. Rev. Lett. **70**, 4026 (1993).
[22] C.O. Reinhold, M. Melles, H. Shao, and J. Burgdörfer, J. Phys. B **26**, L659 (1993).
[23] F. Robicheaux, Phys. Rev. A **56**, R3358 (1997); **60**, 431 (1999).
[24] G. Duchateau, E. Cormier, and R. Gayet, Eur. Phys. J. D **11**, 1991 (2000).
[25] G. Duchateau, C. Illscas, B. Pons, E. Cormier, and R. Gayet, J. Phys. B **33**, L571 (2000).
[26] N.A. Papadogiannis, B. Witzel, C. Kalpouzos, and D. Charalambidis, Phys. Rev. Lett. **83**, 4289 (2000).
[27] P. Corkum, Nature (London) **403**, 845 (2000).
[28] M. Nilsoli, S. de Silvestri, O. Svelto, R. Szipöcs, K. Ferencz, Ch. Spelmann, S. Sartania, and F. Krausz, Opt. Lett. **22**, 522 (1997).
[29] S. Geltman, J. Phys. B **33**, 1967 (2000).
[30] N. Austern, Y. Iseri, M. Kamimura, M. Kawai, G. Rawitscher, and M Yahiro, Phys. Rep. **154**, 126 (1987).
[31] G. Schiwietz, Phys. Rev. A **42**, 296 (1990).
[32] L. Kocbach and I. Ladadwa, Nucl. Instrum Methods Phys. Res. B (to be published).
[33] H.M. Nilsen and J.P. Hansen, Phys. Rev. A **63**, 011405(R) (2001).
[34] J. Zhang and P. Lambropoulos, J. Phys. B **28**, L101 (1995).
[35] C.O. Reinhold and C.A. Falcón, Phys. Rev. A **33**, 3859 (1986).
[36] L.I. Schiff, *Quantum Mechanics*, 3rd ed. (McGraw-Hill, Singapore, 1968), p. 289.
[37] J.N. Bardsley, A. Szöke, and J.M. Comella, J. Phys. B **21**, 3899 (1988).
[38] E. Cormier and P. Lambropouos, J. Phys. B **29**, 1667 (1996).
[39] E. Cormier and P. Lambropoulos, Eur. Phys. J. D **2**, 15 (1998).
[40] P. Dietrich, F. Krausz, and P. Corkum, Opt. Lett. **25**, 16 (2000); M. Mehendale, S.A. Mitchel, J.P. Likforman, D.M. Villeneuve, and P. Corkum, *ibid.* **25**, 1672 (2000).
[41] http://www.fi.uib.no/ nilsen/movies